Indian Journal of Engineering & Materials Sciences
Vol. 33, February 2026, pp. 111-125
DOI: 10.56042/ijems.v33i01.23968

Evaluating the effects of carbon black from recycled tires on subgrade stabilization, pavement design, and construction-phase CO_2 emissions

Tacettin Geçkil & Bahadır Karabaş*
Department of Civil Engineering, Faculty of Engineering, Inonu University, 44280 Malatya, Turkey

Received: 18 September 2025; accepted: 11 January 2026

This study has investigated the effects of subgrade stabilization using carbon black (CB) derived from recycled vehicle tires on the pavement structure, and subsequently on sustainability based on CO_2 emissions during the initial construction of the road. Soil samples (A-6 class per AASHTO) have been prepared with CB additions of 0%, 2.5%, 5%, 10%, 15%, and 20%. Tests have determined the optimal CB ratio as 10%, leading to 28%, 77%, and 186% increases in CBR values after 1, 7, and 28 days, respectively. Pavement thickness and costs have been designed using AASHTO 1993, showing that the best results depending on the curing times have been achieved with a 30.44% reduction in flexible pavement thickness and a 26.08% decrease in unit area cost, while rigid pavement thickness and unit area cost have been reduced by 9.67%. For a 1000 m × 20 m road, the most favorable cost savings depending on the curing times have been estimated at USD 62,890 for flexible pavement and USD 24,052 for rigid pavement. Sustainability analysis has indicated that the optimal outcomes depending on the curing times have included CO_2 reductions of 25.91% and 9.33% for flexible and rigid pavements, respectively, mainly due to material production, which has accounted for 67% and 95% of total emissions.

Keywords: AASHTO method, Carbon black, Carbon footprint, Soil, Stabilization, Sustainability

1 Introduction

In our evolving world, structures like buildings, dams, bridges, and highways are designed across diverse terrains, climates, and soil types. A critical aspect of this process is evaluating soil properties, which may not always meet design requirements for strength, permeability, and compressibility. When relocating a project is impractical, soil stabilization becomes essential to enhance these properties, ensuring structural safety and minimizing economic risks[1,2].

The improvement of road subgrades is essential in regions where highways are extensively used. Enhancing low-bearing-capacity soils as road base materials reduces pavement costs and increases safety. Stabilization methods include mechanical (mixing soils for better grading) and chemical (adding pozzolanic materials like lime, cement, or fly ash) techniques[2]. Recently, recycled materials such as blast furnace slag, fly ash, and rice husk ash have been incorporated into stabilization efforts. Over the past 20 years, several studies have reported significant soil improvements: Muhhotar and Hantoro[3] increased the CBR from 3.03% to 16.3% using 6% lime and 12.5% rice husk ash. Basha *et al.*[4] raised clay soil CBR up to 60% with 5% rice husk ash and 4% cement. Alhassan and Mustapha[5] enhanced unconfined compression strength and CBR by adding 2-8% cement and 4-6% rice husk ash to laterite soil. Okafor and Okonkwo[6] increased laterite soil CBR from 22.05% to 80.14% with 10% rice husk ash. Brooks[7] improved clay soil CBR by 47% and compression strength by 97% using 12% rice husk ash and 25% fly ash. Sakr *et al.*[8] noted a sevenfold strength increase in soft clay with 7% lime over 60 days. Choobbasti *et al.*[9] found higher CBR values with 4% lime and 3-5% rice husk ash in low plasticity silt. Yadu *et al.*[10] reported a 50-190% compression strength rise in black cotton soil using 12% fly ash and 9% rice husk ash. Other studies showed improvements in silty sand[11], clay[12], and swelling clay soils[13] using combinations of lime, rice husk ash, cement, and pond dust. Kumar S.N *et al.*[14] increased CBR 1.2-1.5 times with 6% carbon black. G. Bharti *et al.*[15] reported a 50% rise in unconfined compression strength with 20% copper slag in black cotton soil.

Recent studies have utilized various waste and recycled materials for soil stabilization, with growing emphasis on environmental sustainability. Sustainability aims to meet present needs without

*Corresponding author (E-mail: karabasbaha@gmail.com)

compromising future generations[16], making it essential to assess and mitigate the environmental impact of engineering applications. A major focus is reducing greenhouse gas emissions, particularly CO_2, which constitutes 95% of total emissions[17]. In 2020, Turkey's greenhouse gas emissions reached 523.9 million tons of CO_2 equivalent, with transportation contributing 15.3% (80.680 kilotons)[18]. Given these figures, analyzing the carbon footprint of highway design and construction is crucial for sustainable transportation. In light of these figures, it is evident that researching the carbon footprint, focusing on the analysis of greenhouse gas emissions, is crucial for evaluating the sustainability of highway design and construction activities within the broader context of transportation activities. Rogers *et al.*[19] compared crushed stone and lime-stabilized soil layers in highway design, focusing on emissions. Giustozzi *et al.*[20] found that cement stabilization could cut emissions by over 80%, advocating its use. Gupta *et al.*[21] reduced CO_2 emissions from 910.9 to 750.8 tons/km in a four-lane road using a stabilizing additive. Zhang *et al.*[22] reported a 57.09% emission reduction by using lime-stabilized soil and geogrid-reinforced embankments. Kaewunruen *et al.*[23] analyzed the carbon footprint of the Beijing-Shanghai high-speed railway, identifying construction as the largest contributor (64.86%) and stressing the need for eco-friendly technology.

Each year, approximately 17 million tons of waste tires are generated globally, often incinerated or stored in open areas, causing environmental damage and posing economic challenges due to storage costs and fire risks. Despite their use in various recycling applications, particularly pyrolysis[24], there is limited research on the effects and sustainability of using carbon black (CB), a byproduct from waste tires, to stabilize road bases.

This study investigates the impact and sustainability of stabilizing road subgrades with CB through experimental tests and calculations. Pure soil and CB-stabilized soil samples were tested using sieve analysis, hydrometer, consistency limits, picmometer, standard proctor, unconfined compression and CBR tests. Based on CBR results, road pavement thicknesses were calculated using the AASHTO 1993 method, and pavement costs were assessed. Sustainability was analyzed through carbon footprint calculations, evaluating CO_2 emissions during the construction phase (material production, transportation, machinery use) for flexible and rigid pavements with both pure soil and CB-stabilized subgrades.

2 Materials and Methods

2.1 Materials

The soil sample from Inonu University Campus underwent sieve analysis (ASTM C136/C136M), hydrometer analysis (ASTM D422-63), Atterberg limits (ASTM D4318), and standard Proctor tests (ASTM D698), classifying it as A-6 and SC according to AASHTO and Unified Soil Classification. The plasticity index was 11.31%, with a plastic limit of 14.56%, a liquid limit of 25.87%, and a grain unit volume weight of 2.71 g/cm³. Figure 1 shows the particle size distribution curves.

Carbon Black (CB), a stabilizing additive, is produced from recycled tires via pyrolysis, a heat-driven process in an oxygen-free environment. This results in fine, black, water-insoluble particles. The pyrolysis process involves gasification, condensation, and the extraction of CB, which is odorless, has a self-ignition temperature above 140°C, and a density of 1.7-1.9 g/cm³[25].

Figure 2, Fig. 3 and Fig. 4 present scanning electron microscopy (SEM) images, X-ray diffraction (XRD) and fourier transform infrared spectroscopy (FTIR) patterns of the soil and CB used in the study, respectively.

When the SEM images in Fig. 2 are examined, it is seen that the SC soil has an irregular and rough surface with particles of various sizes and shapes. It has also been determined that it has a plate like structure due to its clay content. The CB additive material appears to have an irregular granular structure with variable particle sizes.

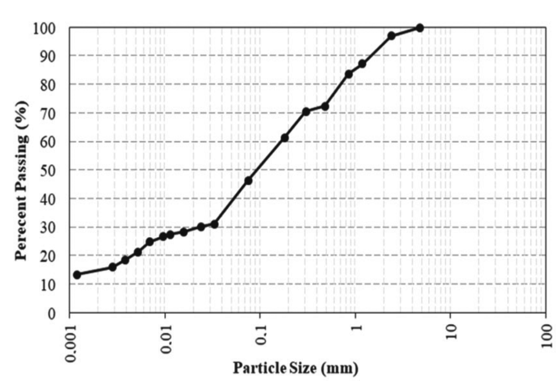

Fig. 1 — Particle size distribution curves of the soil.

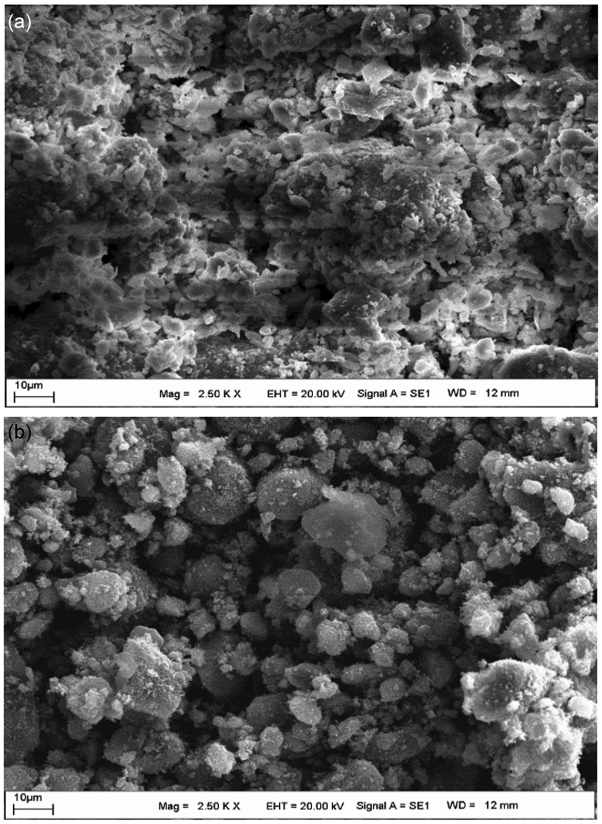

Fig. 2 — SEM images of the materials (a) Pure soil and (b) CB.

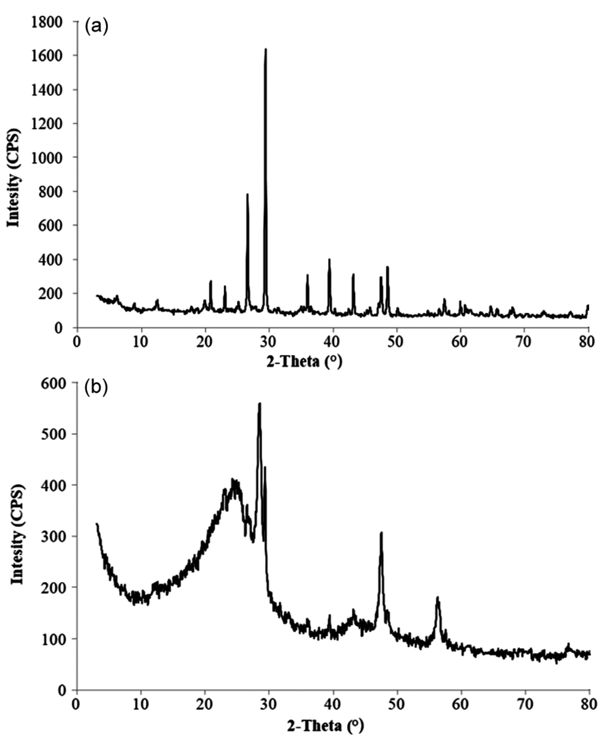

Fig. 3 — XRD patterns of the materials (a) Pure soil and (b) CB.

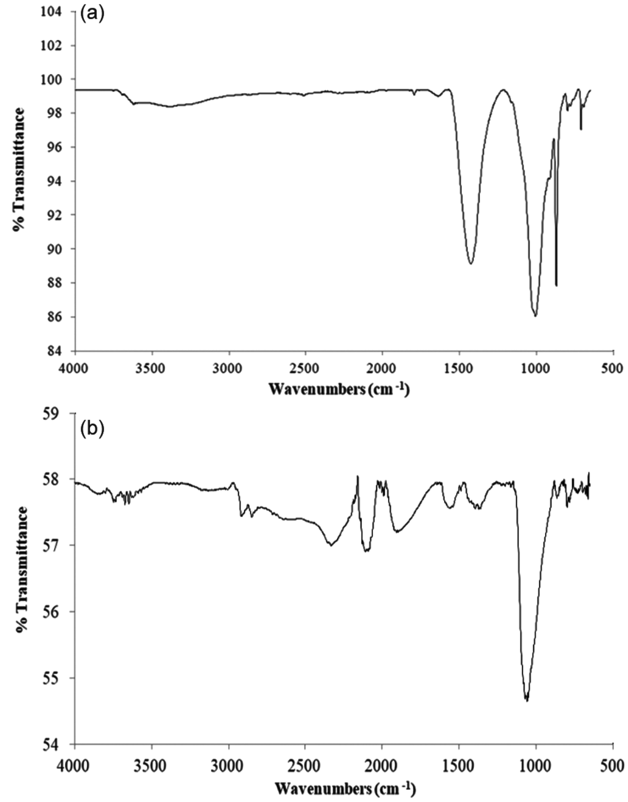

Fig. 4 — FTIR patterns of the materials (a) Pure soil and (b) CB.

Figure 3 reveals the primary distinguishing peaks for both substances. When examining the SC soil via XRD, a noticeable peak in the vicinity of 2θ ≅26 - 29° on the plot signifies the existence of silica (SiO_2), while the wide and weak peak zones imply a clay-like formation. The emergence of varied peaks is attributed to the makeup of soils containing sand and clay. In the CB's XRD evaluation, a diffused peak region spanning roughly 2θ ≅20° to 2θ≅25° implies that the carbon black possesses a non-crystalline arrangement. Furthermore, the peak at 2θ ≅48° is believed to denote the occurrence of graphitic material. The diminished strength of the CB peak reinforces the existence of graphite.

When the FTIR graph in Fig. 3 is examined, it is evaluated that the peak around 1000-1100 cm^{-1} of the SC soil indicates Si-O-Si stretching, supporting the presence of SiO_2. Additionally, it is evaluated that the peaks around 1400-1500 cm^{-1} and 870 cm^{-1} indicate carbonate (CO_3^{2-}) asymmetric stretching vibration. The CB additive material, with its composition of 50.64% carbon, 46.62% oxygen, 2.12% hydrogen, and 1.62% sulfur, indicated C-O structures with the largest peak around 1100 cm^{-1}. Furthermore, it is

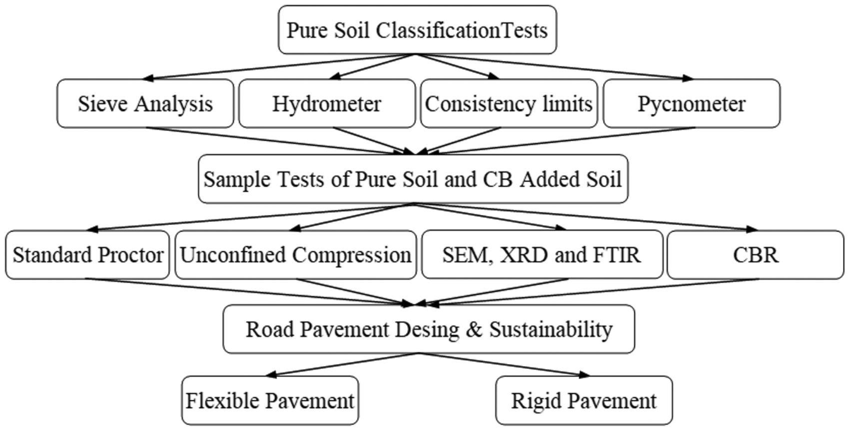

Fig. 5 — Flow chart.

Fig. 6 — (a) and (b) Applications of the experimental tests, (c) and (d) Standard proctor test, (e) Unconfined compression test, (f) and (g) CBR test.

evaluated that the peaks around 1600 cm^{-1} and 2100 cm^{-1} may be related to carbon-carbon or carbon-oxygen bond extensions.

2.2 Methods

2.2.1 Preparation of samples

After determining the properties of the soil sample (SC), the optimal water content (ω_{opt}) and maximum dry unit weight (γ_{kmax}) were found using the standard Proctor test (ASTM D698). Mixtures containing 2.5%, 5%, 10%, 15%, and 20% CB by weight were tested. Unconfined compression test samples were prepared with the same ω_{opt} and γ_{kmax} ratios and evaluated for strength after curing for 1, 7, and 28 days. CBR samples were also tested for CBR values following ASTM D1883-13. All procedures (Fig. 5) adhered to relevant test standards.

2.2.2 Experimental method

The standard Proctor test (ASTM D698) determines the maximum dry unit weight and optimum water content of a soil sample[26]. The unconfined compression test (ASTM D2166) measures the uniaxial compressive strength of soil samples[27]. The California bearing ratio (CBR) test (ASTM D1883) assesses soil bearing capacity by analyzing the load-penetration relationship[28]. Figure 6 has shown the applications of the experimental tests, including (a) and (b) Standard Proctor test, (c), (d), and (e) unconfined compression test, and (f) and (g) CBR test. The chemical properties of the materials and mixtures were analyzed using scanning electron microscopy (SEM) for surface morphology, X-ray diffraction (XRD), fourier transform infrared spectroscopy (FTIR) for structural properties, including crystalline and amorphous characteristics[29].

2.2.3 Design

The highway structure consists of infrastructure (the shaped road section) and pavement (sub-base, base, and surface layers) designed to bear traffic loads. Design factors such as soil condition, traffic flow, regional aspects, and economics influence layer thickness and project lifespan[30]. This study includes both flexible and rigid pavement design.

2.2.3.1 Design of flexible road pavement with AASHTO method

The AASHTO Method (1993) designs flexible pavement with asphalt cement as a binder, typically consisting of pavement, base, and sub-base layers. The pavement layer includes the wearing course, binder, and bituminous base, with materials like bitumen and aggregate[30]. Figure 7 shows the layers of flexible pavement.

Layer thicknesses are calculated using Equation 1, according to AASHTO (1993) Design Guidelines[30].

$$\log(W_{8.2}) = Z_R \times S_0 + 9.36 \times \log(SN+1) - 0.20 + \frac{\log\left(\frac{\Delta PSI}{4.2-1.5}\right)}{0.40+\frac{1094}{(SN+1)^{5.19}}} + 2.32 \times \log M_R - 8.07 \quad \ldots (1)$$

Here, $W_{8,2}$ represents the 8.2 tons equivalent standard single axle load repetition (project traffic), M_R is the resilient modulus of subgrade soil (psi), S_0 is the combined standard error of traffic and performance forecast, Z_R is the standard normal deviation, SN is the structural number (inches), and ΔPSI is the difference between initial (Po) and final service (Pt) capability index. After calculating SN using Equation 1, the thicknesses of flexible pavement layers are determined using Equation 2, incorporating layer coefficients[30].

$$SN = a_1 \times D_1 + a_2 \times D_2 \times M_2 + a_3 \times D_3 \times M_3 \ldots a_i \times D_i \quad \ldots (2)$$

In this equation, D_1, D_2, and D_3 represent the thicknesses of the pavement, base, and sub-base layers, while a_1, a_2, and a_3 are their relative strength coefficients, and M_2, M_3 are drainage coefficients for the base and sub-base layers, considered as 1.00 for calculating flexible pavement thicknesses. These coefficients are provided in AASHTO 1993. After the flexible pavement layer thicknesses were determined, the layer thicknesses were checked by calculating the SN* values given in Fig. 8.

2.2.3.2 Design of rigid road pavement by AASHTO method

In rigid pavement design using the AASHTO Method (1993), a concrete slab made with portland cement is placed directly on the subgrade. Determining appropriate thicknesses for the concrete slab and layers is crucial to withstand deformations from heavy traffic. Figure 9 shows a cross-sectional view of the rigid pavement and its layers.

According to AASHTO (1993) guidelines, layer thicknesses are calculated using Equation 3[30].

$$\log_{10}(w_{8,2}) = Z_R . S_0 + 7.35.\log_{10}(d+1)$$
$$0.06 + \frac{\log_{10}\left[\frac{\Delta PSI}{4.2-1.5}\right]}{1+\frac{1.624.10^7}{(d+1)^{8.46}}} + (4.22-0.32.Pt).$$
$$\log_{10}\left[\frac{S'c.Cd\,(d^{0.75}-1.132)}{215.63.J\left[d^{0.75}\frac{18.42}{(Ec/k)^{0.25}}\right]}\right] \quad \ldots (3)$$

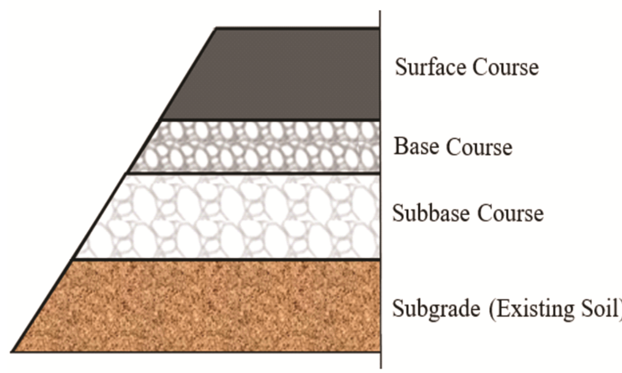

Fig. 7 — Flexible pavement sectional view.

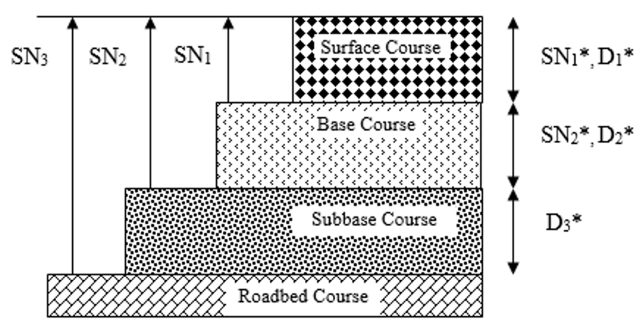

Fig. 8 — Pavement numbers in flexible pavement[31].

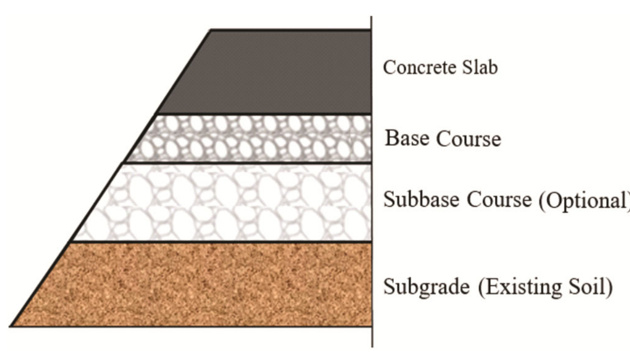

Fig. 9 — Rigid pavement section view.

Here; $W_{8.2}$=8.2 tons equivalent standard single axle load repetition number (project traffic), ZR=Standard normal deviation, So=Combined standard error of traffic forecast and performance forecast, d=Thickness of concrete pavement (inches), ΔPSI=The difference between the initial design service capability (Po) and the final service capability index (Pt), S'c=Modulus of rupture for concrete (psi), J=Load transfer coefficient, Cd=Drainage coefficient, Ec=Modulus of elasticity of concrete (psi), and k=Modulus of subgrade reaction (psi). The design utilized an optimal stabilizer mixture to maximize strength and evaluate its impact on rigid pavement. It followed the criteria for joint unreinforced concrete pavement and complied with the Turkish Highways Concrete Pavement Design Guidelines

2.2.4 Sustainability analysis

Highway design employs soil stabilization with cement, lime, and bitumen. Recycled and waste materials are increasingly considered for their cost-effectiveness, but sustainability requires assessing their CO_2 emissions[32]. While technical and economic factors are important, greenhouse gas analysis is crucial. International efforts like the 1992 Framework Convention on Climate Change and the 1997 Kyoto Protocol highlight the global focus on reducing greenhouse gas emissions[33]. CO_2, accounting for approximately 95% of human-caused greenhouse gas emissions, is the major driver of global warming. Following the Kyoto Protocol's phases, the 2015 Paris Agreement established the post-2020 climate framework. Recent conferences, including the 2024 UAE meeting, have led to a significant agreement to move away from fossil fuels[34-35].

The Intergovernmental Panel on Climate Change (IPCC) method, based on the 2006 methodology, is used globally for calculating CO_2 emissions. Reviews in 1996, 2006, and 2019 reaffirmed the 2006 method's sound foundation, making major revisions unnecessary[36-38] Turkey also utilizes this method in its 2024-2030 Climate Change Mitigation Strategy and Action Plan[39]. The method for calculating CO_2 emissions uses three "Tier" levels, each based on pre-set average values. Tier 1, utilizing energy consumption from fuel combustion, is suitable for construction emission estimates. Tier 2, focused on vehicle combustion technology, is used in specific vehicle emission control applications. Tier 3 is applied for in-depth analysis of the transportation sector[36-38].

This study compared flexible and rigid pavement designs, using CBR values from unstabilized and carbon black-stabilized soil. Layer thicknesses were determined using the AASHTO 1993 method. The carbon footprint was calculated for a 1000m x 20m divided road, including the stabilized layer. The sustainability analysis focused on initial construction, assessing CO_2 emissions from material production, transportation, machinery, and equipment.

2.2.4.1 Calculation of CO_2 emissions for road construction

Flexible pavement's bituminous hot mix (HMA) consists of 93-97% aggregate and 3-7% bitumen, the latter acting as a binder[31]. This study calculates CO_2 emissions from HMA production, using estimated values of 190 kg/ton[40] for bitumen and 6.5 kg/ton[20] for aggregate. Water usage emissions are excluded 0.3 kg/ton[20]. The assumed unit volume weight of the pavement material is 2.4 tons/m3. Rigid pavements utilize a Portland cement concrete slab over a granular base. Concrete production involves cement, aggregates, water, and admixtures. Cement is a significant CO_2 emitter, contributing 7-8% globally and 12-13% in Turkey. Clinker production, a cement component, has nearly equivalent CO_2 emissions. Aggregate emissions come from quarry extraction and crushing. Mineral additives, used as cement substitutes, are by-products and don't emit CO_2. For this study[41], C35/45 concrete was selected per Turkish guidelines, with an estimated CO_2 emission of 339.57 kg/m^3. Carbon black produced via pyrolysis emits approximately 518 kg of CO_2 per ton. When used as a stabilizer in road base stabilization, it is recycled from end-of-life tires through pyrolysis, which yields approximately 35–40% carbon black[25,42]. End-of-life tires are often incinerated as fuel, generating between 647 and 2270 kg of CO_2 per ton during combustion[42–45]. In the current calculation, the avoided CO_2 emissions are estimated as $0.35 \times (647 + 2270) / 2 = 510$ kg/ton, representing a negative carbon footprint. This value is based on the average CO_2 emissions from tire combustion, assuming that 35% of each tire is converted into carbon black through the pyrolysis process.

This study used the Tier 1 approach[37,38] to calculate CO_2 emissions from road construction materials (concrete, bitumen, aggregate) and a stabilizer (carbon black) for a sample road. Emissions were determined using Equation 4, based on CO_2 emission factors per unit volume (kg/m³) or mass (kg/ton).

$E_{CO_2} = DA \times FE$ … (4)

Here; E_{CO_2} = Total CO_2 emission (kg), DA = Activity Data (TJ) (TJ: Activity Data Unit tons or kg) FE = Emission Factor (kg/TJ) (unit CO_2 emission amount) DA = Material supplied for the construction of the sampled road (weight for stabilization and flexible pavement) or (volume for rigid pavement).DA = l x b x h x γ ; l = length of the path (m), b = width of the road (m), h = depth of the road (m), and γ ;= unit volume weight of road construction materials (ton/m^3 if FE value is kg/ton). Unit volume weight will be used to calculate the weight of stabilization and flexible pavement.

2.2.4.2 Calculation of CO_2 emissions caused by transportation, machinery and euipment in road construction

This study calculated CO_2 emissions from flexible pavement construction, including layers like wearing, binder, bituminous base, granular base, subbase, and carbon black-stabilized road base. The analysis accounted for material production, transportation (using a 10-ton truck over 50km), and on-site processes like paving, compaction, and spraying. Specific equipment and procedures for each layer were considered. Transportation emissions were calculated using 2.96 kg CO_2/ton[21], and total emissions were determined using Equation 4. This study assessed CO_2 emissions from rigid pavement construction (concrete slabs) and carbon black-stabilized road base, focusing on transportation, machinery, and equipment. Concrete transport used 6.5m^3 transit mixers (9.5 kg CO_2/m^3, 50km)[41,46,47], while stabilizer transport utilized 10-ton trucks (2.96 kg CO_2/ton, 50km)[21,41,47]. On-site processes like paving, compaction, and curing were considered. Machinery emissions were calculated using fuel consumption data from the Turkish GDH and a modified equation (Equation 6), comparing standard and carbon black-stabilized road base construction. Equation 4 was used for transportation calculations.

$$F = BSFC.\ P.\ T.\ 1\ /\ \gamma \qquad \text{… (5)}$$

$$\varepsilon_{CO2} = F.\ \alpha \qquad \text{... (6)}$$

Here; F = Fuel Consumption (L), BSFC = Brake specific fuel consumption (g/(kW.h)), P = Motor power at the rotational speed that provides the maximum torque (kW), T = Time (hour), γ = Density of fuel used (0.832 kg/L). ε_{CO2} = Total CO_2 emission (kg), α = CO_2 emitted when consuming 1 liter of diesel (2.6639 kg/L)[20].

3 Results and Discussion

This study investigated the effects and sustainability of carbon black (CB) stabilized road base soil in highway pavements. Standard Proctor and unconfined compression tests were performed on pure soil and CB-reinforced samples after 1, 7, and 28 days of curing. CBR tests were conducted on samples with the optimal 10% CB ratio. Using the CBR results, flexible and rigid pavement layer thicknesses were designed according to the AASHTO 1993 method, and pavement costs were calculated. Sustainability analyses, assessment based on CO_2 emissions, were performed for both pure soil and CB-stabilized designs.

3.1 Standard proctor and unconfined compression test results

Standard Proctor tests (ASTM D698) were conducted on pure soil and soil samples with 2.5%, 5%, 10%, 15%, and 20% carbon black (CB) additives. The results, shown in Fig. 10, indicate that as the CB ratio increased, the optimum water content (ω_{opt}) increased, while the maximum dry unit volume weight (γ_{kmax}) decreased. This is attributed to CB's granular and hollow chain structure[48], which increased the mixture's absorption capacity[14], aligning with previous research. Unconfined compression tests were performed on soil samples prepared using the ω_{opt} and γ_{kmax}. Samples were tested after 1, 7, and 28 days of curing. Test results for different curing times is shown in Figs 11 and 12.

Unconfined compression tests showed that increasing carbon black (CB) concentration and curing time enhanced soil compressive strength. The 10% CB samples had the highest strength, showing significant increases (82%, 114%, 142%) over pure soil after 1, 7, and 28 days. While CB enhances hardness and shear resistance, exceeding 10% might decrease tensile strength[49]. The observed decrease in unit strain with increased CB is due to the hardness increase, consistent with literature[50] that hard soils have lower strain in unconfined compression tests.

3.2 CBR test results

CBR samples, both pure soil and 10% carbon black (CB) additive, were prepared using the optimal quantity identified from unconfined compression test results. The samples were cured for 1, 7, and 28 days in a controlled environment. After curing, dry CBR

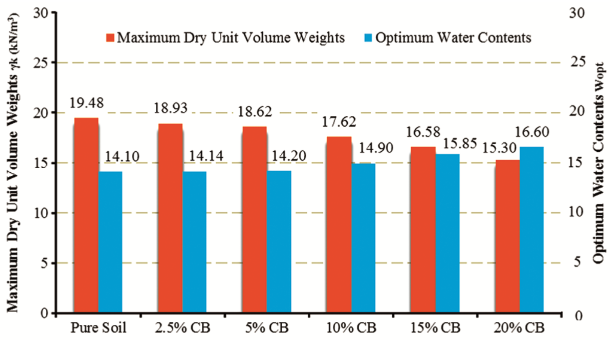

Fig. 10 — Standard proctor test results.

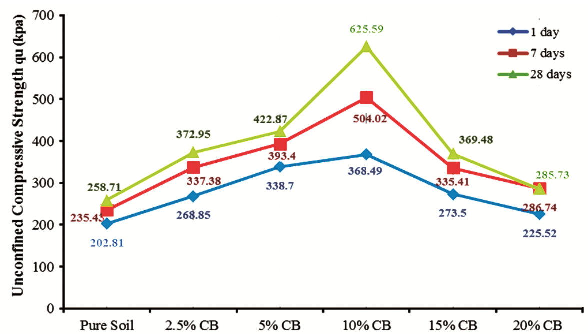

Fig. 11 — Change of UCS values depending on additive ratio and curing time.

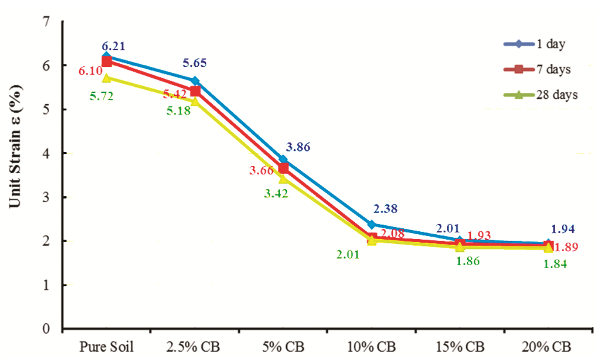

Fig. 12 — Change of unit strain depending on additive ratio and curing time.

tests were conducted, and the resulting CBR values are shown in Fig. 13. CBR tests showed significant increases in strength for carbon black (CB) stabilized soil compared to pure soil, with increases of 21%, 47%, and 132% for 2.5mm penetration, and 28%, 77%, and 187% for 5mm penetration, after 1, 7, and 28 days of curing, respectively. The 10% CB samples exhibited higher CBR values with longer curing times, demonstrating CB's positive impact on soil cohesion and internal friction due to its fine particle and amorphous structure, consistent with prior research. The obtained results support the literature[14,51,52].

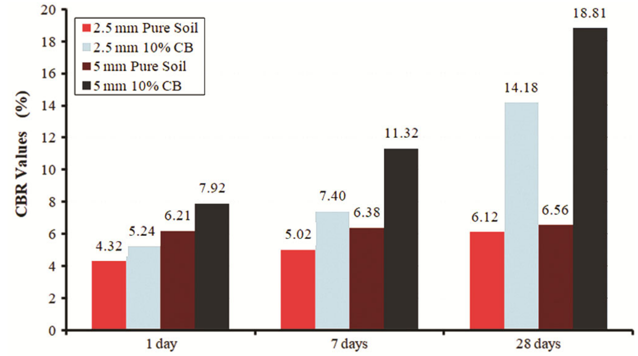

Fig. 13 — Change of CBR values depending on curing time.

3.3 SEM, XRD, FTIR test results

As a result of the experiments conducted in the study, the optimum mixture ratio was determined as 10% CB by adding CB to the soil samples at different ratios. SEM images prepared to observe the effect of CB in the mixtures prepared with different ratios of CB are given in Fig. 14, XRD and FTIR analyses prepared to explain the stabilization mechanism of the optimum improvement occurring with 10% CB are given in Fig. 15.

When the SEM images are examined, it is observed that a more compact and crack-free structure occurs at the optimum additive ratio. It is evaluated that the limited effect of the CB amount at the ratios before the optimum additive ratio is due to this. In mixtures with ratios higher than the optimum additive ratio, it is confirmed by the presence of unreacted particles that the excess additive material could not react and therefore did not produce a positive effect.

When the XRD pattern is examined, it is evaluated that the peaks seen around $2\theta \cong 26° - 29°$ indicate the presence of quartz (SiO_2). It is thought that the peaks seen around $2\theta \cong 40° - 50°$ are due to the amorphous structure and graphite content of the carbon black. When the FTIR graph is examined, it is appreciated that the peak around 1000 cm^{-1} causes the stretching of Si-O bonds and indicates the SiO_2 structure. It is evaluated that the peaks around 1500 cm^{-1} and 3500 cm^{-1} may be due to the gel structure formed as a result of the significant impact of the clay minerals in the soil due to stabilization.

3.4 Flexible pavement design

This study utilized maximum CBR values obtained after 1, 7, and 28 days of curing for pure soil and 10% carbon black (CB) added soil to design flexible pavements according to AASHTO 1993 guidelines. The resilient modulus (M_R) was estimated using the formula

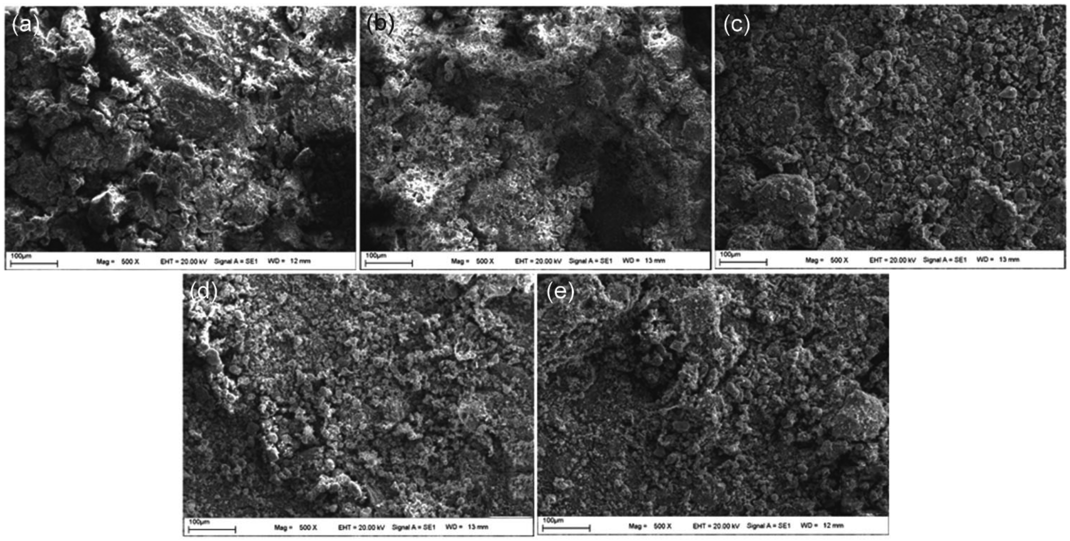

Fig. 14 — SEM images of additive soil samples (a) 2.5% CB, (b) 5% CB, (c) 10% CB, (d) 15% CB and (e) 20% CB.

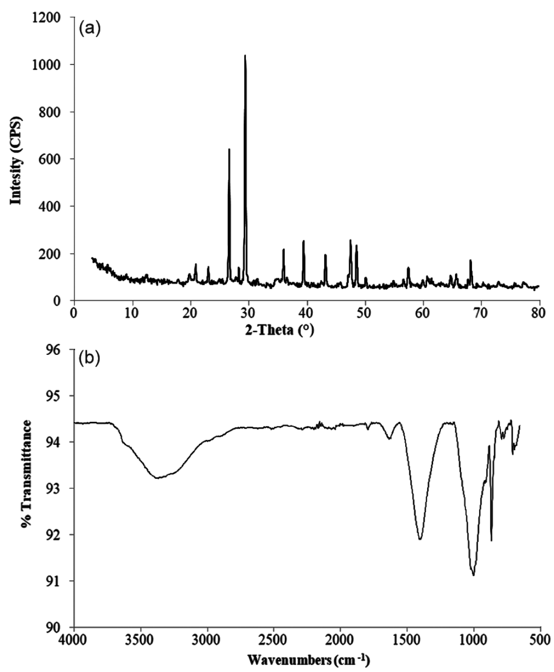

Fig. 15 — (a) XRD and (b) FTIR patterns of the samples %10 CB.

M_R = 1500 x CBR. Calculated[53] M_R values for pure soil were 9315, 9570, and 9840 psi, and for 10% CB additive soil, they were 11880, 16980, and 28215 psi, corresponding to the respective curing periods. Total pavement layer thicknesses were calculated using Equation 1, incorporating common values from Table 1 and resilient modulus (M_R) values. Table 2 shows that, compared to pure soil, the layer thicknesses decreased by 8.45%, 14.29%, and 30.44% for the carbon black-stabilized soil at different curing times.

3.5 Economic analysis of flexible pavement

This study analyzed the economic impact of carbon black-stabilized soil on highway flexible pavement costs using 2025 unit price data from the Turkish General Directorate of Highways (Table 3). The Turkish General Directorate of Highways (GDH) provides unit prices for different pavement layers (sub-base, base, bituminous courses). Using these prices, the study conducted a cost analysis and created a comparison graph (Fig. 16) illustrating flexible pavement unit costs based on soil sample curing times.

Flexible pavement construction costs with 10% carbon black (CB) stabilized soil decreased by 5.85%, 17.93%, and 26.08% per unit m² compared to pure soil, depending on curing times. For a 1000m x 20m divided road, this translates to savings of USD 14200, USD 43400, and USD 63000 for 1, 7, and 28-day curing periods, respectively.

3.6 Rigid pavement design

Rigid pavement design followed AASHTO 1993 guidelines, comparing pure soil and 10% carbon black (CB) added soil. Unreinforced jointed pavement thickness was calculated using maximum CBR values after 1, 7, and 28 days of curing, with C35/45 concrete class. M_R and modulus of subgrade reaction (k) were determined using established relationships (M_R = 1500 x CBR and k = M_R / 19.4[30,53]) and parameters from Table 4.

Calculated modulus of subgrade reaction (k) values for pure soil were 480.15, 493.30, and 507.22 psi, and for 10% carbon black (CB) added soil were 612.37, 875.26, and 1454.38 psi, for 1, 7, and 28 days of curing, respectively. Using these k values and Table 5

Table 1 — Parameters used in flexible pavement calculation.

Parameters	Selected value
Equivalent standard axle load repetition number, $W_{8,2}$	60000000
Combined standard error of traffic forecast and performance forecast, S_0	0.45
Initial service index of road, P_0	4.2
Final servicea index of road, Pt (For motorways, state roads 2.5)	2.5
Total loss of service capability, ΔPSI	1.7
Standard normal deviation, Z_R (R=%95)	-1.645

Table 2 — Layer thicknesses selected for different curing times of pure soil and %10 CB. soils.

Layer type	Layer thickness (cm)					
Wearing course	5	5	5	5	5	5
Binder course	8	7	8	7	8	5
Bituminous base course	12	12	12	8	12	8
Granular base	20	16	20	15	20	15
Sand-gravel subbase	26	25	25	25	24	15
Total layer thicknesses	71	65	70	60	69	48
Subgrade soils	Pure Soil	10% CB	Pure Soil	10% CB	Pure Soil	10% CB
CBR (%)	6.21%	7.92%	6.38%	11.32%	6.56%	18.81%
CBR curing times (days)	1		7		28	

Table 3 — 2025 GDH unit costs of layer thicknesses[54].

Item number	Definition	Unit	Unit price (USD)	m^2 /cm (USD)
KGM/6405/S	5 cm Wearing course	m^2	2.53	0.51
KGM/ 6305	5 cm Binder course	m^2	1.94	0.39
KGM/ 6307	7 cm Binder course	m^2	2.68	0.38
KGM/ 6308	8 cm Binder course	m^2	3.05	0.38
KGM/ 6208	8 cm Bituminous base course	m^2	2.90	0.36
KGM /6212	12 cm Bituminous base course	m^2	4.31	0.36
KGM/6040	Granular base	m^3	7.83	0.08
KGM/6010	Sand-gravel subbase	m^3	2.59	0.03

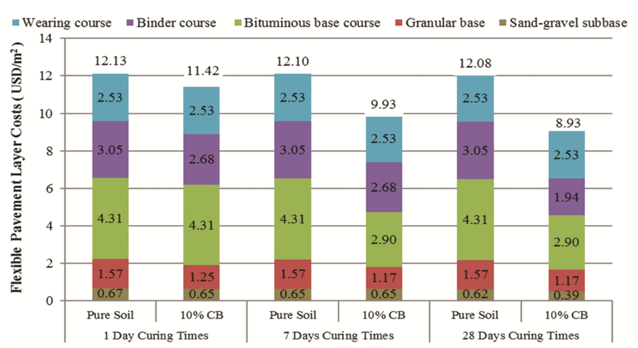

Fig. 16 — Flexible pavement layer costs calculated for pure and soils additive with 10%CB.

parameters, rigid pavement layer thicknesses were calculated with Equation 3. Pure soil required thicknesses of 30.99, 30.84, and 30.71 cm (rounded to 31 cm), while 10% CB-additive soil required 30, 29, and 28 cm, respectively. The rigid pavement layer thicknesses for pure soil and 10% CB additive soils exposed to different curing times are given in Table 5. It was found that the pavement layer thicknesses for soils additive 10% CB decreased by 3.23%, 6.45% and 9.67%, respectively, compared to pure soil.

3.7. Rigid pavement economic analysis

This study evaluated the cost impact of carbon black-stabilized soils on highway rigid pavement construction, using GDH criteria and 2025 MoEU unit price schedules for C35/45 concrete. Table 6 presents the calculated unit costs (per m²) for rigid pavement, and Fig. 17 visually compares these costs for different curing times (1, 7, and 28 days) of soil samples.

Rigid pavement construction costs with 10% carbon black (CB) stabilized soil decreased by 3.23%, 6.45%, and 9.67% per unit m² at different curing times. For a 1000m x 20 m divided road, this resulted in savings of USD 8000, USD 16000, and USD 24200, respectively, depending on the curing periods.

3.8 Flexible pavement sustainability analysis

This study assessed CO_2 emissions for flexible pavement designs with pure soil and carbon black-

Table 4 — Parameters used in rigid pavement calculation.

Parameters	Selected value
Equivalent standard axle load repetition number, $W_{8,2}$	60000000
Load transfer coefficient, J	2.7
Drainage coefficient, Cd	1
Modulus of rupture of concrete (psi), S'c	660
Compound standard error of traffic forecast and performance forecast, S_0	0.35
Initial service index, P_0	4.5
Final service index of road, Pt (For motorways, state roads 2.5)	2.5
Total loss of service capability, ΔPSI	2
Modulus of elasticity of concrete, Ec (C 35/45)	4786244
Standard normal deviation, Z_R (R=%95)	-1.645

Table 5 — Selected layer thicknesses of 1, 7 and 28 day cured soil samples.

Layer type	Layer thickness (cm)					
C35/45 concrete layer	31	30	31	29	31	28
Subgrade soils	Pure Soil	10% CB	Pure Soil	10% CB	Pure Soil	10% CB
CBR (%)	6.21%	7.92%	6.38%	11.32%	6.56%	18.81%
CBR curing times (days)	1		7		28	

Table 6 — 2025 unit cost of layer thickness in rigid pavement design[55].

Item number	Definition	Unit	Unit price (USD) (USD)	m^2/cm (USD)
151.501.007	C35/45 Concrete Layer	m^3	40.03	0.40

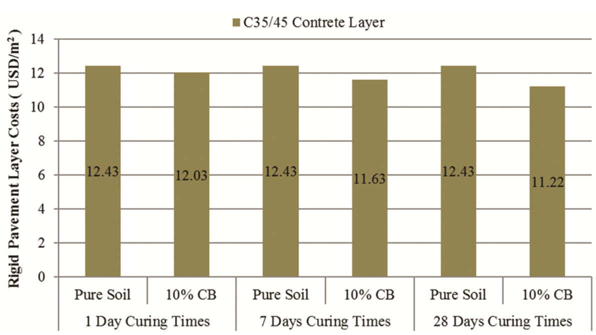

Fig. 17 — Rigid pavement layer costs calculated for pure and 10%CB additive soil.

stabilized soil, using Equations 4 and 6. Material production and transportation emissions were calculated, assuming 5% bitumen and 95% aggregate in bituminous layers and 10% carbon black stabilization (a depth of 30 cm). Pure soil emissions were 313680, 310950, and 308220 kg CO_2, while 10% CB-stabilized soil emissions were 292506, 259680, and 217332 kg CO_2. Including stabilizer material reduced CO_2 emissions by 4.06%, 13.77%, and 26.75% for 1, 7, and 28-day curing periods, respectively.

CO_2 emissions from transportation, machinery, and equipment in flexible pavement construction were calculated using GDH fuel consumption data. For pure soil, emissions were 157437, 156114, and 154791 kg CO_2 for 1, 7, and 28-day curing. With 10% CB stabilization, emissions decreased to 154600, 138203, and 117244 kg CO_2, resulting in reductions of 1.8%, 11.47%, and 24.26%, respectively. Further reductions are possible through optimized transportation and fuel-efficient machinery. Emission details for pure and CB-stabilized soils are in Tables 7 and 8, and a comparative analysis by strata is in Fig. 18.

Total CO_2 emissions for pure soil flexible pavement were 471,117, 467,064, and 463,011 kg for 1, 7, and 28-day curing. With 10% carbon black (CB) stabilization, emissions decreased to 455,554, 406,331, and 343,024 kg, resulting in reductions of 3.30%, 13%, and 25.91%, respectively. Material production accounts for 66–67% of total emissions, highlighting the benefits of reducing pavement layer thickness, which varies depending on the curing time. These findings align with existing literature[20,21].

3.9 Rigid pavement sustainability analysis

This study analyzed CO_2 emissions for rigid pavements using pure and carbon black (CB)-stabilized subgrade soils on a 1000m x 20m road. Equations 4 and 6 were used for material/transportation and machinery emissions, respectively. Calculations focused on concrete slabs and CB-stabilized road base, adhering to GDH guidelines for unreinforced concrete pavement[56]. Reinforcement emissions were excluded due to consistent

Table 7 — The emission quantities specific to CB on road base soil.

Layer type	Th	CB (ton)	A CO_2 (kg/ton)	A Footprint CO_2 (kg)	RE CO_2 (kg/ton)	RE Footprint CO_2 (kg)	SS Footprint CO_2 (kg)	B CO_2 (kg/ton)	B Footprint CO_2 (kg)	C CO_2 (kg/m^3)	C Footprint CO_2 (kg)
Soils Stabilized 10%CB	30	1056	518	547008	510	-538560	8448	2.96	3126	1.570953	4712.86
						Total	8448		3126		4712.86

Th: Layer Thicknesses (cm), (A) Carbon Footprint from the Production of CB Materials CO_2 (kg and kg/ton), (RE) Recycling Emission Carbon Footprint from the Production of CB Materials CO_2 (kg and kg/ton), (SS) Carbon Footprint from the Soils Stabilized CO_2 (kg), (B) Carbon Footprint from the Transportation of CB Materials CO_2 (kg and kg/ton). (C) Carbon Footprint from Soils Stabilized the Machinery and Equipment CO_2 (kg).

Table 8 — Flexible pavement emission amounts for pure and 10%CB additive base soils.

The emission from according to layer thickness

Layer type	Days	Pure Soil				10% CB			
		Th	A CO_2 (kg)	B CO_2 (kg)	C CO_2 (kg)	Th	A CO_2 (kg)	B CO_2 (kg)	C CO_2 (kg)
Wearing course	1	5	37620	7104	12504	5	37620	7104	12504
Binder course	1	8	60192	11366	19552	7	52668	9946	17108
Bituminous base course	1	12	90288	17050	28022	12	90288	17050	28022
Granular base	1	20	54600	24864	2579	16	43680	19891	2064
Sand-gravel subbase	1	26	70980	32323	2073	25	68250	31080	1993
Total		**71**	**313680**	**92707**	**64730**	**65**	**292506**	**85071**	**61691**
Wearing course	7	5	37620	7104	12504	5	37620	7104	12504
Binder course	7	8	60192	11366	19552	7	52668	9946	17108
Bituminous base course	7	12	90288	17050	28022	8	60192	11366	18681
Granular base	7	20	54600	24864	2579	15	40950	18648	1935
Sand-gravel subbase	7	25	68250	31080	1993	25	68250	31080	1993
Total		**70**	**310950**	**91464**	**64650**	**60**	**259680**	**78144**	**52221**
Wearing course	28	5	37620	7104	12504	5	37620	7104	12504
Binder course	28	8	60192	11366	19552	5	37620	7104	12220
Bituminous base course	28	12	90288	17050	28022	8	60192	11366	18681
Granular base	28	20	54600	24864	2579	15	40950	18648	1935
Sand-gravel subbase	28	24	65520	29837	1913	15	40950	18648	1196
Total		**69**	**308220**	**90221**	**64570**	**48**	**217332**	**62870**	**46536**

Th: Layer Thicknesses (cm), Days: Curing times, (A) Carbon Footprint from the Production of Materials (Aggregate and Bitumen) CO_2 (kg), (B) Carbon Footprint from the Transportation of Materials (Aggregate and Bitumen) CO_2 (kg). (C) Carbon Footprint from the Machinery and Equipment (Aggregate and Bitumen) CO_2 (kg).

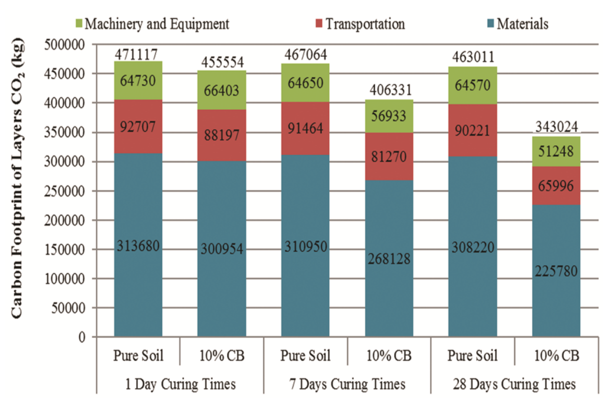

Fig. 18 — Carbon footprint CO_2 comparison chart for flexible pavement.

dimensions. With a 10% CB-stabilized 30cm road base, pure soil emissions were 2105334 kg CO_2, while 10% CB-stabilized soil emissions were 2037420 kg, 1969506 kg, and 1901592 kg for 1, 7, and 28-day curing, respectively.

CO_2 emissions from transportation, machinery, and equipment in rigid pavement production were calculated using GDH fuel consumption data. Concrete was transported by 6.5m³ transit mixers, and carbon black (CB) by 10-ton trucks, both over 50km. The CB-stabilized layer was 30cm thick. Pure soil emissions were 121093 kg CO_2. For 10% CB-stabilized soil, emissions were 125025,

Table 9 — Rigid pavement emission amounts for pure and 10% CB additive base soils.

Layer type	Days	Pure Soil: Th	Pure Soil: A CO_2 (kg)	Pure Soil: B CO_2 (kg)	Pure Soil: C CO_2 (kg)	10% CB: Th	10% CB: A CO_2 (kg)	10% CB: B CO_2 (kg)	10% CB: C CO_2 (kg)
		The emission from according to layer thickness							
C35/45 Contrete Layer	1	31	2105334	58900	62193	30	2037420	57000	60187
	7	31	2105334	58900	62193	29	1969506	55100	58181
	28	31	2105334	58900	62193	28	1901592	53200	56175

Th: Layer Thicknesses (cm), (A) Carbon Footprint from the Production of Materials (Conrete) CO_2 (kg), (B) Carbon Footprint from the Transportation of Materials (Conrete) CO_2 (kg). (C) Carbon Footprint from the Machinery and Equipment (Conrete) CO_2 (kg).

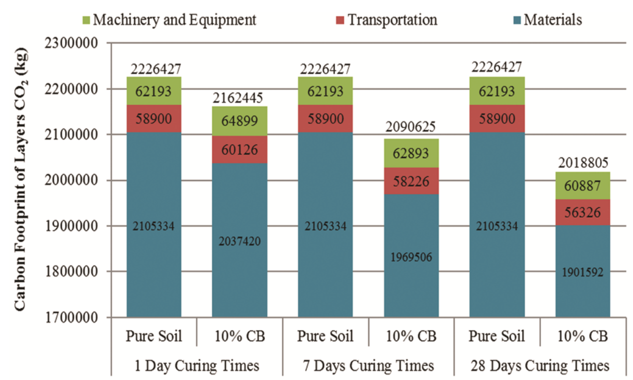

Fig. 19 — Carbon footprint CO_2 comparison chart for rigid pavement.

121119, and 117213 kg CO_2 for 1, 7, and 28-day curing, respectively, with a 3.2% reduction at 28 days. Emission details are in Table 9, and a comparative graph is in Fig. 19.

Total CO_2 emissions in rigid pavement production were 2226427 kg for pure soil and 2162445, 2090625, and 2018805 kg for 10% carbon black (CB)-stabilized soil, corresponding to 1, 7, and 28-day curing. CB stabilization reduced emissions by 2.87%, 6.10%, and 9.33%. Material production constitutes 94–95% of total emissions, emphasizing the importance of reducing pavement thickness to lower CO_2 emissions, which varies depending on the curing time. The findings are consistent with existing research. Furthermore, the consistency of the emission amount weight with the literature[20,21] underscores the reliability of the findings.

4 Conclusion

This study investigated the effects and sustainability of carbon black (CB)-stabilized road subgrade on highway pavement. The results from laboratory experiments, pavement design, and the subsequent sustainability analysis based on CO_2 emissions during the initial construction of the road are summarized below.

a According to the Proctor test results, it was observed that as the amount of CB increased, the water content of the stabilized soil increased and the dry unit volume weight decreased. It is evaluated that CB being fine-grained and lighter compared to pure soil reduces the maximum dry unit volume value.

b Unconfined compression test results showed that CB improved the cohesion of the weak soil and increased its strength, and the highest strength value was obtained from samples containing 10%CB. It was determined that, the strength value of pure soil, with the addition of 10%CB, increased by 82%, 114% and 142% after 1, 7 and 28 days of curing periods, respectively.

c According to the CBR test results, it was determined that adding 10%CB to the soils increased the CBR values of the soils by 28%, 77% and 186% at the end of 1, 7 and 28 days of curing periods, respectively. This change shows that CB has a very improving effect on the bearing capacity of the soil.

d SEM imaging revealed that the optimal additive ratio resulted in a more compact, crack-free structure. XRD analysis confirmed tindicated the amorphous nature of carbon black with graphitic content. FTIR analysis , 1500 cm^{-1} and 3500 cm^{-1} may be attributed to a gel structure formed due to the interaction between clay minerals and the stabilizer.

e According to flexible pavement design and cost analyses, by using 10%CB in stabilization, total layer thicknesses decreased by 8.45%, 14.29% and 30.44%, and unit costs decreased by 5.85%, 17.97% and 26.04%, respectively, depending on the curing times. According to these reductions in unit costs, considering current prices, 14183 USD, 43491 USD and 62890 USD will be saved for an sample road, respectively.

f According to the analysis carried out for rigid pavement design, it was determined that by using

10%CB in stabilization, the total layer thickness and road unit area costs decreased by 3.23%, 6.45% and 9.67%, depending on the curing time. According to these results, it was determined that 8017 USD, 16035 USD and 24052 USD savings could be achieved, respectively. The savings appear to be more significant in the flexible pavement design.

g As a result of the sustainability analysis, it was determined that stabilizing the subgrade with 10% CB for a sample road reduced CO_2 emissions in the flexible pavement design by 3.30%, 13%, and 25.91%, respectively, depending on the curing times. In the rigid pavement design, CO_2 emissions decreased by 2.87%, 6.10%, and 9.33%, respectively, also depending on the curing times.

h It has been observed that in the analyses of flexible and rigid pavements, most of the CO_2 emissions are caused by material production. This ratio ranges between 66–67% for flexible pavement and 94–95% for rigid pavement, depending on the stabilization status of the road subgrade and varying with the curing time. It has also been observed that stabilization can reduce CO_2 emissions by decreasing layer thicknesses in both pavements.

As a result, it has been determined that the use of CB material in ground stabilization significantly reduces flexible and rigid pavement layer thicknesses, construction costs and CO_2 emissions occurring during construction activities. On the other hand, considering that carbon black is obtained as a recycling product from end-of-life vehicle tires, it has been seen that the use of this product in stabilization applications can contribute to the national economy, environmental protection, and mitigation of climate change. In addition, in order to reduce the carbon footprint, it is considered important to minimize material transportation distances, increase studies on different stabilization depths, and select the machines and equipment used from environmentally friendly and fuel-saving vehicles.

References

1 Das B M, Principle of Foundation Engineering (Cengage Learning, USA), 7thEdn, ISBN: 978-0495668107, 2011.

2 Nikolaides A, Highway Engineering Pavements Materials and Control of Quality: An International Text Book from A to Z (CRC Press), 2014.

3 Muntohar A S & Hantoro G, *Electron J Geotech Eng*, 5 (2000).

4 Basha E A, Hashim R, Mahmud H B & Muntohar A S, *Constr Build Mater*, 19 (2005) 448.

5 Alhassan M & Mustapha A M, *Leonardo Electron J Pract Technol*, 11 (2007) 47.

6 Okafor F O & Okonkwo U N, *Niger J Technol*, 28 (2009) 46.

7 Brooks R M, *Int J Res Rev Appl Sci*, 1 (2009) 209.

8 Sakr M A, Shahin M A & Metwally Y M, *Geotech Geol Eng*, 27 (2009) 105.

9 Choobasto A J, Ghodrat H, Vahdatırad M J, Fırouzıan S, Bararı A, Torabı M & Bagherıan A, *Front Earth Sci China*, 4 (2010) 471.

10 Yadu L, Tripathi R K & Singh D, *Int J Earth Sci Eng*, 4 (2011).

11 Shabana S, Anshi C, Shamseera P, Shyamili T M, Sruthi V & Suhaira P, *Int J Adv Eng Technol*, 5 (2014) 55.

12 Gupta D & Kumar A, *J Rock Mech Geotech Eng*, 9 (2017) 159.

13 Karatai T R, Kaluli J W, Kabubo C & Thiong'o G, *J Constr Eng Manage*, 143 (2017).

14 Kumar S N, Reddy A S & Kumar P V, *Int J Sci Technol Res*, 8 (2019) 1817.

15 Bharti G, Hurukadli P & Shukla B K, *Mater Today Proc*, (2023).

16 TechBrief, *Pavement Sustainability*, FHWA-HIF-14-012, (2014).

17 Morita Y, Shimizu K, Kato H, Shibahara H & Ymasaki T, *Joint Rail Conference, JRC*, (2011) 453.

18 Republic of Türkiye Ministry of Environment, Urbanisation and Climate Change, *Ministry Environmental Indicators*, 2025.

19 Rogers C D F, Thomas A M, Jefferson I & Gaterell M, *Transp Res Rec*, 2104 (2009) 80.

20 Giustozzi F, Flintsch G W & Crispino M, *Int J Sustain Transp*, 9 (2015) 73.

21 Gupta G, Sood H & Gupta P K, *Indian J Sci Technol*, 10 (2017).

22 Zhang R, Long M & Zheng J, *Adv Civil Eng*, (2019).

23 Kaewunruen S, Sresakoolchai J & Peng J, *Sustainability*, 12 (2020) 206.

24 Rowhani A & Rainey T J, *Energies*, 9 (2016) 2.

25 Green Karbon Black Brochure, https://eracevre.com/pdf/Carbon_BlackBrochure.pdf, 2024.

26 ASTM_D698, *Standard Test Methods for Laboratory Compaction Characteristics of Soil Using Standard Effort*, ASTM International, (2014).

27 ASTM_D2166, *Standard Test Method for Unconfined Compressive Strength of Cohesive Soil*, ASTM International, (2016).

28 ASTM_D1883, *Standard Test Method for California Bearing Ratio (CBR) of Laboratory-Compacted Soils*, ASTM International, (2016).

29 Liu Y, Wu K, Zheng Y, Lu H, Liu W, Zhang H & Sun Y, *J Build Eng*, 99 (2025) 111566

30 AASHTO, *Interim Guide for Design of Pavement Structures*, Washington D.C, (1993).

31 Highways Flexible Pavement Project Design Guide, *Technical Research Department Pavement Branch*, Ankara, (2008).

32 Correia A G, Winter M G & Puppala A J, *Transp Geotech*, 7 (2016) 21.

33 Kyoto Protocol, https://unfccc.int/kyoto protocol, 2024.

34 Paris Agreement, https://unfccc.int/the-paris-agreement, 2024.

35 Republic of Türkiye Ministry of Foreign Affairs, https://www.mfa.gov.tr/paris-anlasmasi, 2024.
36 IPCC Guidelines, *1996 IPCC Guidelines for natural gas inventories*, 3 (1996).
37 IPCC 2006, *2006 IPCC Guidelines for National Greenhouse Gas Inventories*, IGES Japan, (2006).
38 IPCC 2019, https://www.ipcc.ch/report/2019-refinement, 2024.
39 Republic of Türkiye Ministry of Environment, *Climate Change Mitigation Strategy and Action Plan 2024-2030*, 2024.
40 Safaei M, Oni A O, Gemechu E D & Kumar A, *Fuel*, 256 (2019) 1159.
41 Turkish Ready Mixed Concrete Association, Ready Concrete Life Cycle Guide, (Istanbul), 2021.
42 Yang F, Liang S, Wu H, Yue C, Yan H, Chen X, Zhang J, Yan S & Duan Y, *Ind Eng Chem Res*, 61 (2022) 6512.
43 Tsai W T, Chen C C, Lin Y Q, Hsiao C F, Tsai C H & Hsieh M H, *J Mater Cycles Waste Manag*, 19 (2017) 1288.
44 Valentini F & Pegoretti A, *Adv Ind Eng Polym Res*, 5 (2022) 203.
45 ETRMA, *End of Life Tyres - A Valuable Resource with Growing Potential*, Brussels, (2011).
46 Ağar E, Sütaş İ & Öztaş G, Concrete Roads (Rigid Road Superstructures) (ITU Printing House, Istanbul), 1998.
47 Şanal İ, *Polytech J*, 21 (2018) 369.
48 Macías-García A, Díaz-Díez M A, Alfaro-Domínguez M & Carrasco-Amador J P, *Heliyon*, 6 (2020) e04024.
49 Boonstra B B, *Rubber Technology*, 1 (1973) 51.
50 Uzuner B A, Basic Soil Mechanics (Derya Bookstore, Trabzon), 2020.
51 Geçkil T, Sarıcı T & Karabaş B, *Avrupa Bilim ve Teknoloji Dergisi*, 23 (2021) 222. [In Turkish]
52 Geçkil T, Sarıcı T & Karabaş B, *ECJSE*, 8 (2021) 1372. [In Turkish]
53 Tunç A, Coating Engineering and Applications (Asil Publishing, Ankara), 2004.
54 Turkish General Directorate of Highways, *Unit Prices 2025*, http://www.kgm.gov.tr, 2025.
55 Republic of Türkiye Ministry of Environment, *Unit Prices 2025*, https://yfk.csb.gov.tr, 2025.
56 TCK Concrete Road Pavements Technical Specification, *Turkey*, (2019).